# Hodgkin's Lymphoma
# Cell Classification Report
# draft 2

Lihan Yao

## Introduction

We analyze the dataset of an oncology study centered around Hodgkin's Lymphoma. The format consists of high-resolution microscopy images of tumor tissues under various states of reactivity to the same medical treatment. These tumor tissues and images were procured by the Ingo Mellinghoff Lab at Memorial Sloan Kettering Cancer Center as part of on-going oncology research. A natural machine learning task may be formulated as: given a multi-channel cell image where individual channels correspond to experimentally introduced biological markers, classify the cell between tumor/T-cell types, and if possible, the specific T-cell type.

A central difficulty to this task is the lack of a labeled dataset from which supervised learning traditionally proceeds. With help from MSK oncology researchers, we aim to generate a labeled dataset of 80 samples. We maximize the usage of this human expertise by 1. selecting samples which optimally improved an initial model and 2. applying data augmentation and model architectures specialized in utilizing unlabeled data.

## Data

Due to the exotic nature of tumor cell image data, a central obstacle to training and evaluation has been access to a reliable labeled dataset. In addition, the acquisition of good data has traditionally been the most resource exhaustive component of data science projects. Special care has been taken to maximize the effort of human experts.

Prior to the creation of a labeled dataset, we utilize HALO Image Analysis software for both cell detection (in the form of bounding boxes) and fuzzy labeling. By carefully viewing the tissue site through various biological markers, for a marker $m$, the researcher selected an appropriate threshold $\theta_m$. If a cell's average pixel intensity is above $\theta_m$, it is 'labeled' positive for $m$. This is repeated for 32 biological markers. In this sense, a cell's class can be represented as a 32 dimensional 0/1 vector, and fuzzy, due to this threshold model's inherent variance. To support the on-going oncological research, we concern ourselves with states of four markers in particular. Moreover, we find cells with class vectors which are biologically impossible, but are nontheless informative. For these reasons, a cell may belong to one of five potential classes. See appendix for an explanation of interpreting class labels.

First the ladder network is trained on a large datasets with fuzzy labels generated by the threshold model. This is to distinguish a few hundred difficult samples to present to oncologists.

Figure 1: **Pipeline for cell sample generation from raw images of the study**

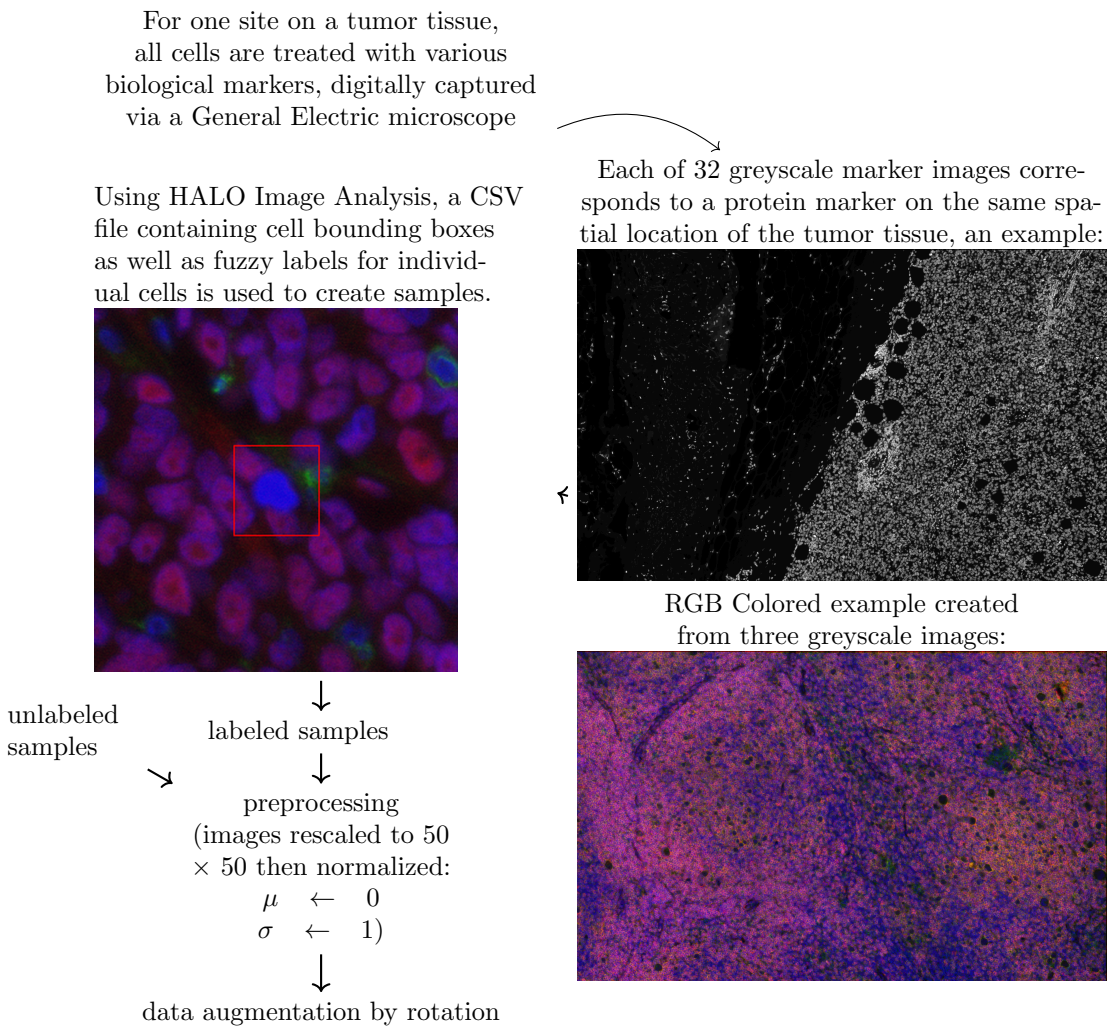


We may then use these labeled samples to evaluate both models and begin a human-labeled dataset. The training set at this stage has 104,500 samples, with test set containing 41,000 and unlabeled set containing 260,800 samples, all after augmentation.

# Model

Model selection is determined by three observations:

1. image samples have high number of channels and high resolution
2. human labeled dataset is a few hundred in size while unlabeled dataset is orders of magnitude

Figure 2: Dimensions of a cell's resultant representation, in a batch

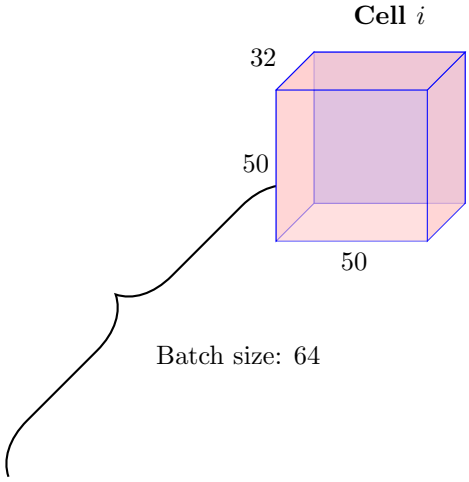


larger.

3. augmenting cell image data by rotatation leads to new data which, to the human eye, is indistinguishable from original data

To take advantage of the last point, we quadruple labeled data by applying right angle rotations to individual samples. This practice was noted in Gao et al. (in the task of HEp-2 Cell Image Classification) to improve the model's rotational invariance. The second point hints at intricate nonlinear relationships which may arise from cell features. This suggests the complexity of a deep net is appropriate for the circumstance. In the area of image classification, ConvNets have been standard.

The first point, mainly that an ideal model should take advantage of the semi-supervised format, has put forth the Ladder Network as most fitting for our task, since it operates an unsupervised denoising task for representation learning, in addition to the original supervised task. To summarize why this works at a high level: the newly introduced denoising cost compells the feedforward layers to find features efficient at generating latent representations close to the posterior distribution. A latent variable is 'pushed' to higher probabilities by our denoising function (learned by layers above).

Parameters of the encoder component (the feedforward component) is detailed below. Each convolutional layer introduces gaussian noise drawn from $\sim \mathcal{N}(\mu, 0.1)$ for the decoder to denoise. Each layer of the encoder learns a representation of the noisy images. During model evaluation, holdout data is passed through these same layers without noise. The decoder reverses the convolutional layers of the encoder by deconvolution and mirrors the encoder configuration.

# Evaluation

At the time of writing, the ladder network has not been trained on human-labeled data. We find that our human-labeled dataset is only sufficiently large for model evaluation, even after data

Table 1: Encoder component of the model

| **Layer Type** | **Kernel** | **Output** | **Stride** | **Activation** | **Notes** |
|---|---|---|---|---|---|
| Conv | 3X3 | 10 | 1 | elu | Batchnorm prior to activation |
| Conv | 3X3 | 20 | 1 | elu | BN |
| Conv | 3X3 | 40 | 1 | elu | BN |
| Conv | 3X3 | 80 | 1 | elu | BN |
| MaxPool | 2X2 | | 2 | | |
| FullyConn | | 5 | | | |

augmentation. The natural baseline to our ladder network is the threshold model whose parameters have been set by researchers via HALO. Though a labeled dataset is absent, we may evaluate the two models by FLOW: an experimental procedure which breaksdown the tumor tissue to classify cell-by-cell. Assuming a model draws samples i.i.d from the population, deviation from FLOW percentages indicates misclassification is occuring. In the columns below, note that a CD4 positive, a CD8 positive cell, or a double positive cell must also be CD3 positive.

Table 2: T-Cell types by percentage, computed experimentally and algorithmically

| | **CD3 %** | **CD4 %** | **CD8 %** | **Total Cells Considered** |
|---|---|---|---|---|
| Threshold | 91.7% | 74.5% | 13.6% | 433327 |
| Ladder Network | 76% | 67.1% | 8.4% | 49920 |
| FLOW trial III | 85% | 74.6% | 9.1% | 436585 |
| FLOW trial II | 80.8% | 71.1% | N/A | 434822 |

In another evaluation approach, we select specific cell examples where the two models disagreed, and evaluate them individually by an oncologist.

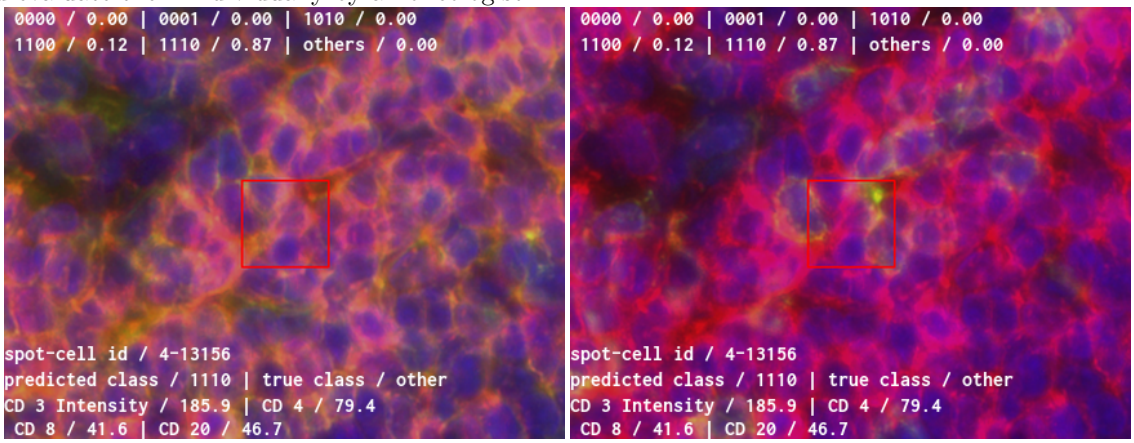


Figure 3: Three channel views of a captioned example where the models disagreed, with Ladder Network's class probabilities listed above

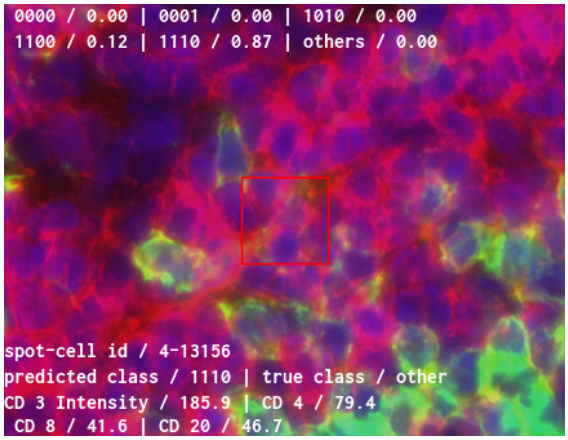


# Discussion and Future Work

We showed initial progress towards a semi-supervised procedure using a dataset with limited label information. The approach employs data augmentation, utilization of vast amounts of unlabeled data, and sample priortization to optimize human labeling. Results of this deep learning model, as evaluated by FLOW and human cell-by-cell classifcation, show improvements over the threshold baseline. There are a variety of directions for future work.

Methods for decreasing the cost of domain-expertise labeling is much needed. As an auxiliary effort, we developed a cell-labeling program complete with keyboard shortcuts, channel view cycling, and image zoom. However, we find that more advanced features such as dynamic image manipulation, i.e. features commonly found in proprietary microscopy image analysis software such as HALO, to be highly helpful in data labeling.

Data augmentation methods beyond rotation should be tried. In the area of cell images, rotated synthetic data satisfies the important property of being indistinguishable from original data to the human eye. Future data augmentation should follow this principle to prevent model performance degradation.

In comparison to a convolutional neural network, the ladder network has at least tripled the computation time for the same number of batches processed. A common operation throughout the network is batch normalization followed by nonlinear activation. An interesting experiment would be to substitute these two steps with a nonlinear activation function that can also implicitly normalize the activations. Very recent developments such as ELU (implemented in the current model alongside BN) and SELU claim to have this property with proper initializations.

# Appendix

## Model Parameter Choices

The first ladder network was worse computationally and performance-wise. The encoder component is detailed below:

Given the complexity of cell images and well known practices from image classification literature, it is better to have a deep network with thin layers. Prior to the development of a ladder network,

| Layer Type | Kernel | Output | Stride | Activation | Notes |
|---|---|---|---|---|---|
| Conv | 3X3 | 20 | 1 | elu | Batchnorm prior to activation |
| Conv | 3X3 | 40 | 1 | elu | BN |
| Conv | 3X3 | 80 | 1 | elu | BN |
| MaxPool | 2X2 | | 2 | | |
| fully-connected | | 5 | | | |

a three layered vanilla ConvNet with batchnorm and dropout was developed (source code found in vanilla_convnet). With threshold labeled data, ConvNet attained 86% accuracy. However the large size disparity between human labeled and unlabeled datasets warranted the added complexity of the ladder network.

Cell segmentation, a common practice in microscopy image analysis, was also tried as a preprocessing step. The procedure zeros out low values in the cell tensor according to a special marker channel which contours the spatial geometry of cell bodies. The overall effect of this procedure is that most pixels outside of the cell membrane have been removed, so as to crop out the central cell. However, this was not used as a preprocessing step because the model suffered additional misclassification following this procedure.

Lastly, an important parameter is the gaussian noise introduced at every encoder layer. As noise increases, the encoder is forced to find more efficient or 'cleaner' representations, since the latent representation passed onto the decoder contains less signal. Experiments show that relative to the MNIST dataset, the tumor cell dataset is much more sensitive to noise. Noise drawn from gaussian distributions with larger variance than $\sim \mathcal{N}(\mu, 0.1)$ not only negatively affects the denoising task, but also supervised classification.

## Interpreting Labels

Some combinations of CD3, CD4, CD8 and CD20 positivity are impossible, but at least one instance of every combination was found in the HALO CSV file. A combination of labels are encoded into binary as follows:

$$\text{CD3 +, CD4 +, CD8 -, CD20 -} \xrightarrow{\text{binary}} \text{`1100}'$$

The first position always correspond to CD3 $+/-$, the second to CD4, and so on.

In confusion matrices, summing over a column such as '0000' yields the number of times our model predicted CD3 -, CD4 -, CD8 -, CD20 -. Summing over a row such as the first one, also corresponding to '000', yields the true number of CD3 -, CD4 -, CD8 -, CD20 - cells.